Advances in Dynamical Systems and Applications
ISSN 0973-5321, Volume 8, Number 1, pp. 125–136 (2013)
http://campus.mst.edu/adsa

Local Mesh Refinement with the PCD Method

Ahmed Tahiri
Université Med Premier
Faculté des Sciences d'Oujda
Département de Mathématiques et Informatique
Av Med VI, BP 717 60000 Oujda, Morocco
tahiriahmed02@yahoo.fr

Abstract

We propose some numerical tests for local mesh refinement using the PCD (piecewise constant distributions) method. The PCD method is a new discretization technique of boundary value problems. It represents the unknown distribution as well as its derivatives by piecewise constant distributions but on distinct meshes. With the PCD method, we can introduce a local mesh refinement without the use of slave nodes. It has the advantage of producing the most compact discrete schemes, even with the presence of a local mesh refinement. Here we investigate some numerical experiments, using local mesh refinement, to show the convergence of the PCD method, the interest of the local mesh refinement and the dependence of the convergence results with the interface boundary.

AMS Subject Classifications: 65N12, 65N15.
Keywords: PCD method, submeshes, approximate variational formulation, local mesh refinement, compact discrete schemes, $O(h)$-convergence rate.

1 Introduction

The PCD method is a new boundary value problem (BVP) discretization method which represents the unknown distribution as well as its derivatives by piecewise constant distributions but on distinct meshes. The only difficulty of the method consists in the appropriate choice of these meshes. Once done, it becomes rather straightforward to introduce an appropriate approximate variational formulation of the exact BVP on this piecewise constant distributions space. With this method we can introduce a local mesh

Received May 7, 2012; Accepted November 14, 2012
Communicated by Delfim F. M. Torres

refinement without the use of slave nodes that appear in some finite element discretizations or in finite volume methods with a local mesh refinement, see [2–4, 8]. Compared with other discretizations, the PCD method has the advantage of producing the most compact discrete schemes, independently of the presence or not of the local mesh refinement. In this paper, we investigate some numerical tests to show the convergence of the presented method, first without local refinement and then with local refinement. Also, we try to illustrate the dependence of the convergence results with the interface boundary. To keep the presentation of this new discretization as simple as possible, we restrict this contribution to the analysis of the 2D diffusion equation on a rectangular mesh with a refined subregion. The convergence analysis and technical results of the PCD method can be found in [5–7].

We consider solving the following BVP on a rectangular domain Ω:

$$-\text{div}(p(x)\nabla u(x)) + q(x)u(x) = s(x) \qquad x \text{ in } \Omega, \tag{1.1}$$

$$u(x) = 0 \qquad x \text{ on } \partial\Omega\,. \tag{1.2}$$

We assume that $p(x)$ is bounded and strictly positive on $\overline{\Omega}$, $q(x)$ is bounded and nonnegative on Ω and we have a well posed problem. We note that the extension of the theory to general boundary conditions does not raise any difficulties. The discrete version of this problem will be based on its variational formulation:

$$\text{find} \quad u \in H \quad \text{such that} \quad \forall\, v \in H \quad a(\,u,\,v\,) = (s,\,v), \tag{1.3}$$

where $H = \{v \in H^1(\Omega), v = 0 \text{ on } \partial\Omega\}$, $(s,\,v)$ denotes the $L^2(\Omega)$ scalar product and

$$a(u,v) = \int_\Omega p(x)\nabla u(x)\cdot\nabla v(x)dx \,+\, \int_\Omega q(x)u(x)v(x)dx. \tag{1.4}$$

2 Preliminaries

2.1 The PCD Discretization

The principle of the PCD method is given in three steps. First, we split the domain Ω under investigation into elements Ω_ℓ such that

$$\overline{\Omega} = \bigcup_{\ell=1}^{M} \overline{\Omega}_\ell\,, \qquad \Omega_k \cap \Omega_\ell = \emptyset \quad \text{if } k \neq \ell.$$

Second, we define different submeshes on each element Ω_ℓ to represent elements of $H^1(\Omega)$ and their derivatives. Third, we require that the discrete representations of elements of $H^1(\Omega)$ must be continuous across the elements boundaries, i.e., along the normal to the element boundary. We denote the representation of $v \in H^1(\Omega)$ by v_h and the representation of its derivatives $\partial_i\, v$ $(i = 1,\, 2)$ by $\partial_{hi}\, v_h$ $(i = 1,\, 2)$. The operators

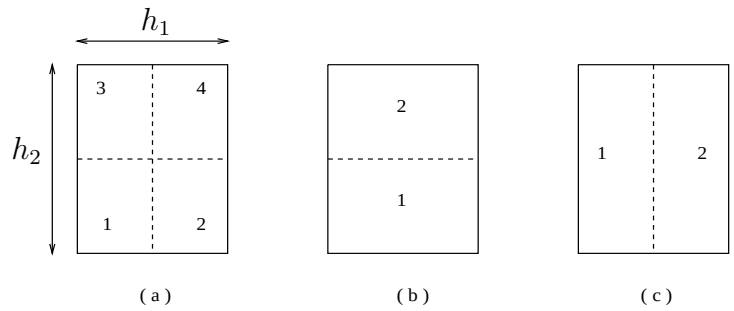

Figure 2.1: Regular element.

∂_{hi} $(i = 1, 2)$ are the finite difference quotients taken along the element edges, in the case of the rectangular elements.

Figure 2.1 gives an example of submeshes used to define $v_h|_{\Omega_\ell}$, $\partial_{h1}\, v_h|_{\Omega_\ell}$ and $\partial_{h2}\, v_h|_{\Omega_\ell}$ on a regular rectangular element Ω_ℓ; $v_h|_{\Omega_\ell}$ is the piecewise constant distribution with 4 values v_{hi} on the regions denoted i $(i = 1, \ldots, 4)$ on Figure 2.1 (a); $\partial_{h1}\, v_h|_{\Omega_\ell}$ is the piecewise constant distribution with constant values:

$$(\, \partial_{h1}\, v_h\,)_1 = \frac{v_{h2} - v_{h1}}{h_1}, \qquad (\, \partial_{h1}\, v_h\,)_2 = \frac{v_{h4} - v_{h3}}{h_1}$$

on the regions denoted 1 and 2 on Figure 2.1 (b). Similarly, $\partial_{h2}\, v_h|_{\Omega_\ell}$ is the piecewise constant distribution with constant values:

$$(\, \partial_{h2}\, v_h\,)_1 = \frac{v_{h3} - v_{h1}}{h_2}, \qquad (\, \partial_{h2}\, v_h\,)_2 = \frac{v_{h4} - v_{h2}}{h_2}$$

on the regions denoted 1 and 2 on Figure 2.1 (c).

In addition, v_h must be continuous across the boundaries of the element. Thus, for example, if the bottom boundary of Ω_ℓ is common with the top boundary of Ω_k, then one must have $v_{h1}(\Omega_\ell) = v_{h3}(\Omega_k)$ and $v_{h2}(\Omega_\ell) = v_{h4}(\Omega_k)$.

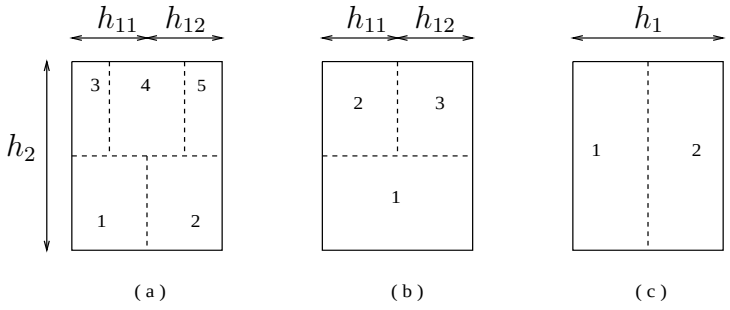

Figure 2.2: Irregular element.

Figure 2.2 gives an example of submeshes used to define $v_h|_{\Omega_\ell}$, $\partial_{h1}\, v_h|_{\Omega_\ell}$ and $\partial_{h2}\, v_h|_{\Omega_\ell}$ in the case of an irregular element, i.e., an element located along the bottom boundary

of the refined zone. In this case $v_h|_{\Omega_\ell}$ assumes 5 values v_{hi}, $i = 1, \ldots, 5$ (Figure 2.2 (a)); $\partial_{h1}\, v_h|_{\Omega_\ell}$ assumes 3 values (Figure 2.2 (b)):

$$(\,\partial_{h1}\, v_h\,)_1 = \frac{v_{h2} - v_{h1}}{h_1}\ , \quad (\,\partial_{h1}\, v_h\,)_2 = \frac{v_{h4} - v_{h3}}{h_{11}}\ , \quad (\,\partial_{h1}\, v_h\,)_3 = \frac{v_{h5} - v_{h4}}{h_{12}}\,,$$

where $h_1 = h_{11} + h_{12}$. Finally, $\partial_{h2}\, v_h|_{\Omega_\ell}$ assumes 2 values (Figure 2.2 (c)):

$$(\,\partial_{h2}\, v_h\,)_1 = \frac{v_{h3} - v_{h1}}{h_2}, \qquad (\,\partial_{h2}\, v_h\,)_2 = \frac{v_{h5} - v_{h2}}{h_2}\,.$$

Also here v_h must be continuous across the element boundaries. Thus, if the top boundary of Ω_ℓ is common with the bottom boundaries of the 2 cells Ω_{k1} and Ω_{k2} of widths h_{11} and h_{12}, we have $v_{h3}(\Omega_\ell) = v_{h1}(\Omega_{k1})$, $v_{h4}(\Omega_\ell) = v_{h2}(\Omega_{k1}) = v_{h1}(\Omega_{k2})$ and $v_{h5}(\Omega_\ell) = v_{h2}(\Omega_{k2})$.

Figure 2.3 (left) provides an example of a rectangular element mesh with a refined zone in the right upper corner. On the same figure we also represent the H_{h0}-mesh used to define globally the piecewise constant distribution v_h. The local mesh refinement is obtained by subdividing the elements (coarse elements), of the zone to be refined, into 4 elements (fine elements). The submeshes defined previously on the regular elements are still valid for the fine elements. The elements are denoted by $\Omega_\ell,\ \ell \in L = \{\,1, \ldots, M\}$ (M is the number of elements). We similarly denote the cells of the H_{h0}-mesh by $\Omega_{\ell 0}$ with $\ell \in J = \{\,1, \ldots, N_G\}$, where N_G is the number of the grid nodes and N denotes the number of unknowns. It is important to note that each node of the mesh may be uniquely associated with a cell of H_{h0}-mesh. We therefore denote them by $N_\ell,\ \ell \in J$. We denote by h the mesh size defined by $h = \max(h_\ell)$, where $h_\ell = \mathrm{diam}(\Omega_\ell)$ $(\ell \in L)$ and we denote by $h_{\ell 1}$ and $h_{\ell 2}$, the width and the height of the element Ω_ℓ. We assume that the discretization is *regular*. We hereby mean that there exist positive constants $C_1,\ C_2 > 0$ independent of h such that:

$$C_1\, h \ \le\ h_{\ell 1}\ ,\ h_{\ell 2}\ \le\ C_2\, h \qquad\qquad \forall\, \ell \in L\ . \tag{2.1}$$

We split the domain Ω into two subdomains Ω_C (the coarse zone) and Ω_R (the refined zone) with $\Omega = \Omega_C \cup \Omega_R$. Finally, we denote by Ω_I the union of all irregular elements, $\Omega_I = \cup_\ell\, \Omega_\ell$ such that $\Omega_\ell \cap \Omega_R = \emptyset$ and $\overline{\Omega}_\ell \cap \partial\Omega_R \neq \emptyset$. The subdomain Ω_I is a strip in Ω with an $O(h)$-width and has the interface boundary as part of its boundary. Before closing this section we note that triangular elements may also be introduced. In this way, the method can accommodate any shape of the domain under investigation through the combined use of a local mesh refinement and triangular elements, see [5]. We note that the use of rectangular and triangular elements is not a restriction of the PCD discretization. Other elements and other forms of submeshes on such elements can be used, see [1]. The notation C is used throughout the paper to denote a generic positive constant independent of the mesh size.

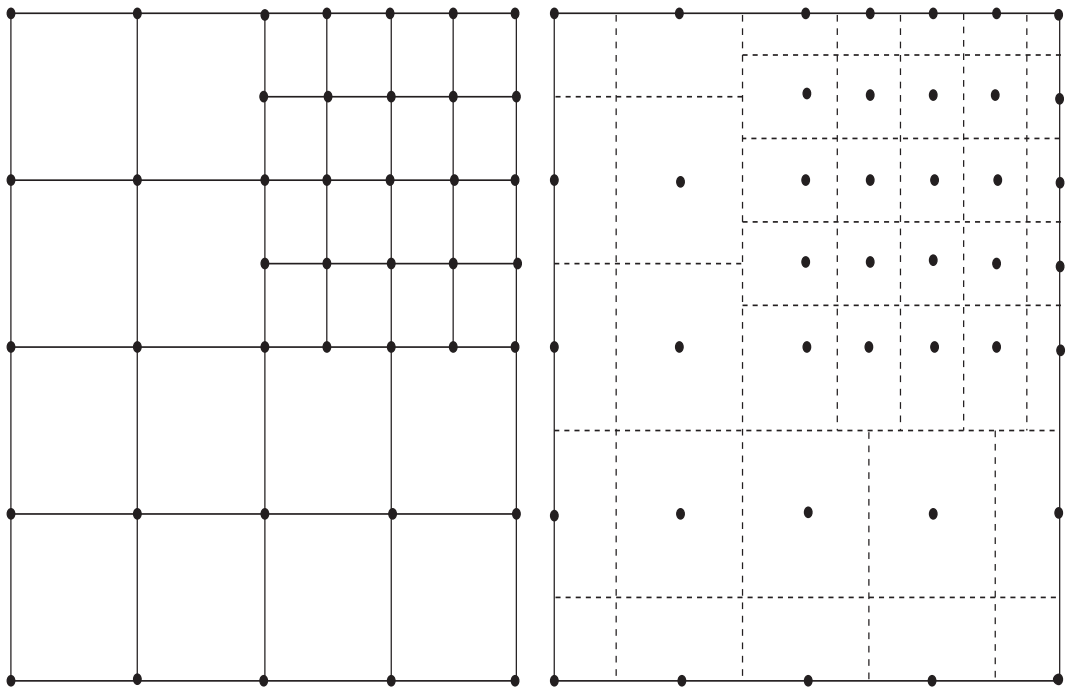

Figure 2.3: Discrete meshes with local mesh refinement.

2.2 Discrete Problem

We denote by H_{h0} the space of piecewise constant distributions used to define v_h equipped with the $L^2(\Omega)$ scalar product. We further denote by H_h the space H_{h0} equipped with the inner product:

$$(v_h , w_h)_h = (v_h , w_h) + (\partial_{h1} v_h , \partial_{h1} w_h) + (\partial_{h2} v_h , \partial_{h2} w_h). \qquad (2.2)$$

The discrete problem to be solved in H_h is defined by:

$$\text{find} \quad u_h \in H_h \quad \text{such that} \quad \forall\, v_h \in H_h \quad a_h(u_h, v_h) = (s, v_h), \qquad (2.3)$$

where

$$a_h(u_h , v_h) = \sum_{i=1}^{2} (p(x) \partial_{hi} u_h , \partial_{hi} v_h)_\Omega + (q(x) u_h , v_h)_\Omega . \qquad (2.4)$$

By introducing the basis $(\phi_i)_{i\in J}$ of the space H_h we get the linear system $\mathcal{A}\,\xi = b$, where $\mathcal{A}$ is the stiffness matrix defined by $\mathcal{A} = (a_h(\phi_j , \phi_i))_{(i,j)\in J}$, b is the vector with components defined by $b_i = (s , \phi_i)_\Omega$ and ξ the unknown vector.

Also, it should be stated that the presented method has the advantage of producing the most compact discrete schemes and the most sparse stiffness matrix resulting from the approximate problem independently of the presence or not of the local mesh refinement. As usual, the error bounds that can be obtained depends on the regularity of u. Here, we assume that $u \in H^2(\Omega)$. In this case, u is continuous on $\overline{\Omega}$ and we can define its interpolant u_I in H_h through

$$u_I(\, N_\ell\,) = \, u(N_\ell) \quad \text{for all nodes } N_\ell\,,\ \ell \in J\,. \tag{2.5}$$

On the other hand, we have shown in [5, 7] the following theoretical results.

Lemma 2.1. *Under the general assumptions and the notations defined above, there exists a positive constant C independent of the mesh size h such that for all v in $H^2(\Omega)$*

$$\left(\|v - v_I\|^2 + \|\partial_1 v - (\partial_{h1} v_I)\|^2 + \|\partial_2 v - (\partial_{h2} v_I)\|^2\right)^{\frac{1}{2}} \leq Ch\|v\|_{2,\Omega}\,, \tag{2.6}$$

where v_I denotes the interpolant of v in H_h.

The result given in the previous lemma is independent of the presence or not of the local mesh refinement.

Theorem 2.2. *Let Ω be a rectangular bounded open set. Assume that the unique variational solution u of* (1.1) *belongs to $H^2(\Omega)$. Then, there exists a constant $C > 0$ independent of h, such that:*

$$\left(\|\, u \,-\, u_h\,\|^2 + \|\,\partial_1\, u \,-\, (\partial_{h1}\, u_h)\,\|^2 \,+\, \|\,\partial_2\, u \,-\, (\partial_{h2}\, u_h)\,\|^2\,\right)^{\frac{1}{2}} \leq\, C\, h\,\|\, u\,\|_{2,\,\Omega}\,,$$

where u_h is the solution of the problem (2.3) *without local refinement.*

Theorem 2.3. *Let Ω be a rectangular bounded open set. Assume that the unique variational solution u of* (1.1) *belongs to $H^2(\Omega)$. Then, there exists a constant $C > 0$ independent of h, such that:*

$$\left(\|\, u \,-\, u_h\,\|^2 + \|\,\partial_1\, u \,-\, (\partial_{h1}\, u_h)\,\|^2 \,+\, \|\,\partial_2\, u \,-\, (\partial_{h2}\, u_h)\,\|^2\,\right)^{\frac{1}{2}} \\ \leq\, C\, h\,\|\, u\,\|_{2,\,\Omega} \,+\, C\, h^{\frac{1}{2}}\,\|\, u\,\|_{2,\,\Omega_I}\,,$$

where u_h is the solution of the problem (2.3) *with a local mesh refinement and Ω_I is a strip in Ω.*

If the solution u is only in $H^1(\Omega)$, then we can still prove the convergence of u_h to u under some assumptions on u on the strip Ω_I, which contains the interface boundary (see [5]).

3 Numerical Experiments

In this section we investigate two numerical examples. In the first one, the solution is very smooth and the mesh does not require a local refinement. This example is considered to illustrate the theoretical results and to establish the dependence factors without any influence from the behavior of the exact solution. In the second example, the exact solution has an anomaly around the center of the domain. This example shows the interest of a local refinement and it also determines the best strategy for such a local refinement.

Sometimes we solve very large problems (very large linear systems) just with the purpose of determining an approximation of the solution in a part of the domain. To this end, we introduce a local error estimator and we try to determine its behavior. We show the contribution of a local mesh refinement to get a better accuracy for this estimator with a lower computational cost.

3.1 Presentation

Consider the problem:

$$-\text{div}\,(\nabla u(x,y)) = s(x,y) \quad \text{in } \Omega \qquad \text{and } \; u(x,y) = 0 \;\text{ on } \partial\,\Omega.$$

We consider the following error estimators: ε_0^r the relative L^2-error estimator and ε_1^r the relative H^1-error estimator defined by:

$$\varepsilon_0^r \;=\; \frac{\|\, u \;-\; u_h \,\|_0}{\|\, u \,\|_0} \quad \text{and} \quad \varepsilon_1^r = \frac{|\,(u_I - u_h)^t\, \mathcal{A}\,(u_I - u_h)\,|^{\frac{1}{2}}}{\|\, u_I \,\|_h} = \frac{\|\, u_I \;-\; u_h \,\|_h}{\|\, u_I \,\|_h}\,,$$

where u is the exact solution of (1.3) and u_I its interpolant in H_h.

The domain under investigation for our examples is $\Omega =]0\,,\,1[\times]0\,,\,1[$. The subregions to be refined are $\Omega_1 = [\,1/4\,,\,3/4\,] \times [\,1/4\,,\,3/4\,]$ and $\Omega_2 = [\,3/8\,,\,5/8\,] \times [\,3/8\,,\,5/8\,]$.

In each example, the approximate mean flux in a subregion $\Omega_F = [\,31/64\,,\,33/64\,]\times [\,31/64\,,\,33/64\,]$ is computed and we try to give the behavior of the error between the exact flux and the computed one. We denote by $|\Omega_F|$ the area of Ω_F, F the exact mean flux in Ω_F and F_h the approximate mean flux in Ω_F. Finally, we denote by η the relative local error estimator defined by:

$$\eta = \frac{|\,F - F_h\,|}{F}\,, \quad \text{where } \; F = \frac{1}{|\Omega_F|}\int_{\Omega_F} u(x)dx \quad \text{and} \quad F_h = \frac{1}{|\Omega_F|}\int_{\Omega_F} u_h(x)dx.$$

We note that the error given in Theorem 2.3 can be written as:

$$\begin{aligned}\big(\|\, u \;-\; u_h \,\|^2 + \|\, \partial_1\, u \;-\; (\partial_{h1}\, u_h)\,\|^2 \;+ \|\, \partial_2\, u \;-\; (\partial_{h2}\, u_h)\,\|^2\,\big)^{\frac{1}{2}} \\ \leq\; C\,h\,\|\, u\,\|_{2,\Omega_C} \;+\; C\,h\,\|\, u\,\|_{2,\Omega_R} \;+\; C\,h^{0.5}\,\|\, u\,\|_{2,\Omega_I}\,, \quad (3.1)\end{aligned}$$

where Ω_C is the coarse zone, Ω_R the refined zone and Ω_I is a strip in the domain Ω with an $O(h)$-width. Thanks to Theorem 2.2 and Theorem 2.3, one may write for the both error estimators ε_0^r and ε_1^r:

$$\max\left(\varepsilon_0^r,\ \varepsilon_1^r\right) \ \leq\ C\,h \qquad \text{without local refinement}$$

$$\max\left(\varepsilon_0^r,\ \varepsilon_1^r\right) \ \leq\ C\,h^{0.5} \qquad \text{with local refinement.}$$

With our numerical investigations, we try to determine numerically the convergence rates of the error estimators defined above.

3.2 Example 1

h^{-1}	N	ε_0^r	ε_1^r	η
8	49	1.908×10^{-2}	1.931×10^{-2}	1.756×10^{-2}
16	225	4.819×10^{-3}	4.891×10^{-3}	3.952×10^{-3}
32	961	1.207×10^{-3}	1.226×10^{-3}	9.639×10^{-4}
64	3969	3.021×10^{-4}	3.069×10^{-4}	2.471×10^{-4}
128	16129	7.554×10^{-5}	7.674×10^{-5}	7.143×10^{-5}
256	65025	1.888×10^{-5}	1.918×10^{-5}	2.088×10^{-5}

Table 1: Example 1, without local refinement.

In this example we choose the source term $s(x,y)$ such that the exact solution is $u(x,y) = x(1-x)y(1-y)$. We have a very smooth solution and we do not need a local refinement. This example is used for theoretical considerations to illustrate the behavior of this method with the local mesh refinement and to illustrate its dependence factors.

From Tables 1–3, we observe a monotonic improvement of the accuracy in both error estimators: they decrease when the mesh size h decreases (when the number of unknowns N increases). That proves the convergence of the presented method independently of the presence or not of a local mesh refinement.

Since the exact solution $u(x,y)$ is very smooth, the presented method has the standard $O(h^2)$-convergence rate for both error estimators with uniform mesh and without local refinement. ε_0^r and ε_1^r are reduced by a factor of 4 when the mesh size is reduced by a factor of 2, see Table 1. Therefore, under higher regularity assumptions, the presented method has the standard $O(h^2)$-convergence rate.

We observe from Tables 2–3, for all refinement cases, that ε_0^r is reduced by a factor of 2 when the mesh size is reduced by a factor of 2. Also, we observe that ε_1^r is reduced by a factor of 2 when the mesh size is reduced by a factor of 4. That proves an $O(h)$-convergence rate for ε_0^r and an $O(h^{0.5})$-convergence rate for ε_1^r. We have a better accuracy with a smaller refined zone (smaller strip and lower number of unknowns)

h^{-1}	N	ε_0^r	ε_1^r	η
8	65	1.768×10^{-2}	6.288×10^{-2}	9.417×10^{-3}
16	281	4.923×10^{-3}	3.538×10^{-2}	2.303×10^{-3}
32	1169	1.543×10^{-3}	2.224×10^{-2}	9.903×10^{-4}
64	4769	5.977×10^{-4}	1.480×10^{-2}	7.760×10^{-4}
128	19265	2.724×10^{-4}	1.014×10^{-2}	4.649×10^{-4}
256	77441	1.326×10^{-4}	7.058×10^{-3}	2.485×10^{-4}

Table 2: Example 1, with local refinement in Ω_2.

than the large zone (large strip and an important number of unknowns). That proves, in absence of any influences, we get better results with smaller strip having the lower length of the interface boundary. Therefore, in these refinement cases, the error bound given in (3.1) is governed by $C\,h^{0.5}\,\|\,u\,\|_{2,\Omega_I}$ (the strip contribution). The better results are obtained with the lower length of the interface boundary. To have a better accuracy we must reduce the impact of this term by reducing the length of the interface boundary.

We note that the local estimator η has nearly the same behavior as the L^2-error estimator ε_0^r in all cases (Tables 1–3). Our numerical results are in agreement with the theoretical results. Moreover, we can improve the estimation of the convergence rate for the L^2-error estimate by $\varepsilon_0^r \leq C\,h$. In the next example, we try to confirm this convergence rate of the L^2-error estimator.

h^{-1}	N	ε_0^r	ε_1^r	η
8	105	2.093×10^{-2}	0.1310	4.371×10^{-2}
16	433	8.707×10^{-3}	8.317×10^{-2}	6.264×10^{-3}
32	1761	4.070×10^{-3}	5.550×10^{-2}	3.001×10^{-3}
64	7105	1.997×10^{-3}	3.807×10^{-2}	1.786×10^{-3}
128	28545	9.941×10^{-4}	2.650×10^{-2}	9.707×10^{-4}
256	114433	4.966×10^{-4}	1.859×10^{-2}	5.014×10^{-4}

Table 3: Example 1, with local refinement in Ω_1.

3.3 Example 2

In this example we choose the source term $s(x,y)$ such that the exact solution is: $u(x,y) = x(1-x)y(1-y)\beta(x,y)$, where $\beta(x,y) = \exp(-100\{(x-0.5)^2+(y-0.5)^2\})$. We have a smooth solution with a sharp peak at the point (0.5, 0.5). This solution varies much more rapidly in Ω_1 than the remaining part of Ω. We have an exponential variation of $u(x,y)$ which starts from the boundary of the subregion Ω_1. Since the exact

h^{-1}	N	ε_0^r	ε_1^r	η
8	49	1.005	0.9599	0.6950
16	225	0.4231	0.5668	0.3918
32	961	0.2219	0.3094	0.2412
64	3969	0.1122	0.1582	0.1036
128	16129	5.631×10^{-2}	7.954×10^{-2}	5.713×10^{-2}
256	65025	2.817×10^{-2}	3.982×10^{-2}	3.092×10^{-2}

Table 4: Example 2, without refinement.

solution $u(x, y)$ has a sharp peak and an important variation in the subregion Ω_1, the presented method cannot have the standard $O(h^2)$-convergence rate using the uniform mesh but only an $O(h)$-convergence rate. We observe that ε_0^r and ε_1^r are reduced by a factor of 2 when the mesh size is reduced by a factor of 2, see Table 4. Comparing the

h^{-1}	N	ε_0^r	ε_1^r	η
8	65	0.4855	0.5824	0.2299
16	281	0.2568	0.3279	2.998×10^{-2}
32	1169	0.1309	0.1799	1.931×10^{-2}
64	4769	6.532×10^{-2}	0.1018	8.403×10^{-3}
128	19265	3.254×10^{-2}	6.114×10^{-2}	4.410×10^{-3}
256	77441	1.623×10^{-2}	3.889×10^{-2}	2.310×10^{-3}

Table 5: Example 2, with local refinement in Ω_2.

results in the Tables 5–6, we obtain better results with a local refinement than the results reported in Table 4 using uniform mesh. The local refinement improves the accuracy of the approximate solution with a lower computational costs. Also in this example, we observe that for all refinement cases, the L^2-error ε_0^r has an $O(h)$-convergence rate and a nearly similar behavior of ε_0^r and η. Table 5 shows that the H^1-error ε_1^r has a nearly an $O(h^{0.5})$-convergence rate (around of an $O(h^{0.65})$-convergence rate). In Table 6, the H^1-error ε_1^r has an $O(h)$-convergence rate even with the local refinement. The argument is that the variation of $u(x, y)$ is entirely located in the zone Ω_1. In other words, the term $\|u\|_{2,\Omega_1}$ in (3.1) is so important that the error estimator ε_1^r depends only on it. Here, the error is only governed by this term that has a very large effect on the error behavior. Unlike than in the previous example, we obtain better results with the large zone Ω_1 that the small zone Ω_2. Moreover, we have an improvement for the local error with this large zone, see column 5 of Tables 5–6 for the estimator η. We explain this by the fact that the variation of the exact solution $u(x, y)$ lies entirely in the subregion Ω_1, unlike than the subregion Ω_2 which contains only a part of this variation. We conclude that the

h^{-1}	N	ε_0^r	ε_1^r	η
8	105	0.3702	0.5127	6.817×10^{-2}
16	433	0.1831	0.2505	2.500×10^{-2}
32	1761	9.352×10^{-2}	0.1271	1.173×10^{-2}
64	7105	4.776×10^{-2}	6.393×10^{-2}	3.243×10^{-3}
128	28545	2.434×10^{-2}	3.205×10^{-2}	7.547×10^{-4}
256	114433	1.233×10^{-2}	1.605×10^{-2}	3.529×10^{-4}

Table 6: Example 2, with local refinement in Ω_1.

best refinement strategy consists in choosing the smallest subregion (to be refined) but it must contains all variations of the exact solution.

4 Concluding Remarks

Using a regular mesh, the theoretical results have shown that an $O(h)$-convergence rate could be derived for the presented method. By introducing a local mesh refinement, the theoretical results have shown that the proposed method presents an $O(h^{0.5})$-convergence rate. The numerical examples presented here are in agreement with these theoretical results. The experimental results have further shown that under higher regularity assumption, the presented method has the standard $O(h^2)$-convergence rate. If the considered problem has an anomaly, then the local refinement gives a better precision, locally and globally, with a lower computational costs. Both theoretical and experimental results show the dependence of the error bounds with the length of the interface boundary. The best refinement strategy consists in choosing the smallest subregion (to be refined) but it must contains all variations of the exact solution. In the case that we have a material discontinuity, discontinuities of the coefficients p or q in (1.1), the zone to be refined must include these material discontinuities. An important conclusion to be drawn from the above experimental results is that the L^2-error has an $O(h)$-convergence rate by using a regular mesh or a locally refined mesh. The perspective of this work is to prove an analogue *Aubin–Nitsche lemma* to justify this L^2-error convergence rate.

References

[1] R. Beauwens, Forgivable variational crimes, in *Numerical methods and applications*, 3–11, Lecture Notes in Comput. Sci., 2542 Springer, Berlin, 2003.

[2] Z. Q. Cai and S. McCormick, On the accuracy of the finite volume element method for diffusion equations on composite grids, SIAM J. Numer. Anal. **27** (1990), no. 3, 636–655.

[3] R. E. Ewing, R. D. Lazarov and P. S. Vassilevski, Local refinement techniques for elliptic problems on cell-centered grids. I. Error analysis, Math. Comp. **56** (1991), no. 194, 437–461.

[4] R. E. Ewing, R. D. Lazarov and P. S. Vassilevski, Local refinement techniques for elliptic problems on cell-centered grids. II. Optimal order two-grid iterative methods, Numer. Linear Algebra Appl. **1** (1994), no. 4, 337–368.

[5] A. Tahiri, A compact discretization method for diffusion problems with local mesh refinement, PhD thesis, Service de Métrologie Nucléaire, ULB, Brussels, 2002.

[6] A. Tahiri, The PCD method, in *Numerical methods and applications*, 563–571, Lecture Notes in Comput. Sci., 2542 Springer, Berlin, 2003.

[7] A. Tahiri, A compact discretization method with local mesh refinement, in press.

[8] P. S. Vassilevski, S. I. Petrova and R. D. Lazarov, Finite difference schemes on triangular cell-centered grids with local refinement, SIAM J. Sci. Statist. Comput. **13** (1992), no. 6, 1287–1313.